MEASUREMENT OF STRAIN FIELDS OF RUBBER BEARINGS BY IMAGE ANALYSIS

University of Tokyo Student Member LEWANGAMAGE Chamindalal Sujeewa
University of Tokyo Member Masato ABE
University of Tokyo Fellow Yozo FUJINO

Introduction

The accuracy of the experimental prediction of material behavior greatly depends on the accuracy of the measurement system. However, the problem is development of accurate and practical measurement systems to acquire data during experiments in order to account for the non-linear behaviors. The measurement of strains fields (more than 10%) in infinitely deformed continua is such a problem since strain gauges are not applicable. Template matching is a widely used method in industrial applications because of the ease of implementation in complex motion detection and pattern recognition problems[1]. Giachetti[2] showed that a correlation based matching technique is suitable for practical measurement of motion. The purpose of this study is to develop correlation-based template matching algorithms to measure the experimental strain fields and trace the localized deformation within the rubber bearings in order to predict the mechanical and failure behavior.

Template Matching

Template matching is a kind of approach to pattern classification. The principle assumptions in this method are that the gray level patterns of pixel blocks can be tracked from one image to the next, that it is constant between successive images and that local texture contains sufficient unambiguous information. Figure 1 shows the deformation of a continuous body within the spatial domain ($M \times N$); two images were taken at time t=0 and t=t. A correlation based matching criterion was used to analyze the gray level pattern around the material points (defined as P) and in the search for the most similar pattern in the successive image. Having defined an initial search window $W(i,j)$ with size ($m \times n$) around the point, we consider similar windows $W(i+p,j+q)$ shifted by the possible integer values in pixels in a search space defined according to the deformation of the body. Normalized correlation (c) of matching was calculated according to equation (1). Sub-pixel level displacements were determined by a Gaussian peak fitting function using correlation data[3]. C1 and C2 are fixed points that are located to scale the deformation, translate and rotate the image according to the un-deformed image. The main routine of matching was written in the C language as shown in Figure 2. Final out put consists of the horizontal and vertical components of displacement vector with respect to the Lagrange co-ordinate system (X,Y).

$$c(p,q) = \frac{\sum_{J=1}^{m}\sum_{I=1}^{n}\{I(i,j)-m_I\}\{I'(i+p,j+q)-m_{I'}\}}{\left[\sum_{J=1}^{m}\sum_{I=1}^{n}\{I(i,j)-m_I\}^2\sum_{J=1}^{m}\sum_{I=1}^{n}\{I'(i+p,j+q)-m_{I'}\}^2\right]^{1/2}} \quad \text{-----------(1)}$$

where $m_I = \frac{1}{nm}\sum_{j=1}^{m}\sum_{i=1}^{n} I(i,j)$ and $m_{I'} = \frac{1}{nm}\sum_{j=1}^{m}\sum_{i=1}^{n} I(i+p,j+q)$

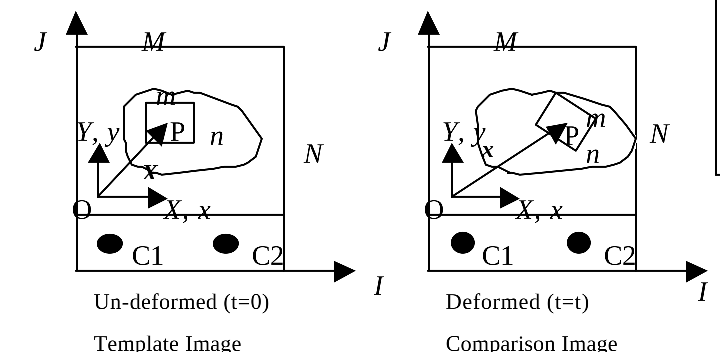

Figure 1: *Template Matching*

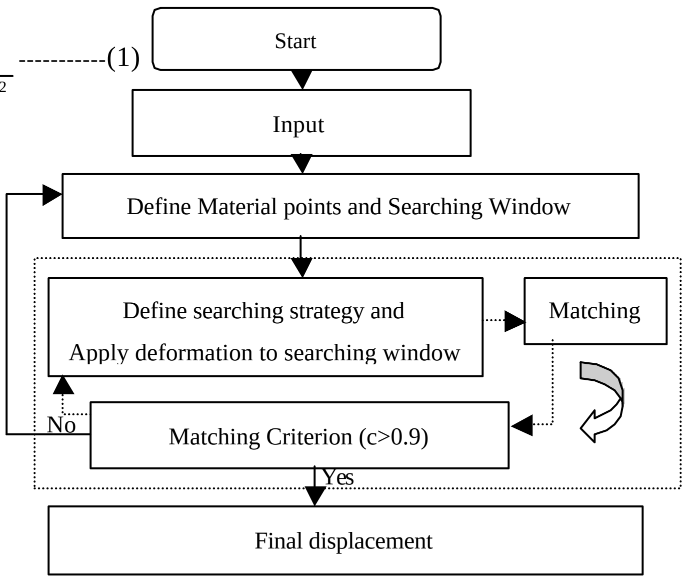

Figure 2: *Flow chart for Matching*

Keyword: Template matching, Displacement fields, Strain fields, Rubber bearings

Address: Hongo 7-3-1, Bunkyo-ku, Tokyo 113-8656, Japan; Tel: 03-5841-6099, Fax: 03-5841-7454
Email: sujeewa@bridge.t.u-tokyo.ac.jp, Masato@bridge.t.u-tokyo.ac.jp, Fujino@bridge.t.u-tokyo.ac.jp

Strain Fields of Rubber bearings

Matching algorithms were applied to obtained the displacement fields of full-scale rubber bearings subjected to combine compression and shear loading. Displacement fields were modified to satisfy the continuity condition (2) assuming that rubber behavior is incompressible. The basic procedure used here is expressing all error displacements ($d\,u^{(k)}$), element coordinates ($\mathbf{x}$) and element displacements ($u^{(k)}$) by form of interpolation functions ($N^{(k)}$) and then an iterative method is used to get a convergent solution. Strain fields can also be obtained expressing all element coordinates and displacements by form of same interpolation functions (3).

$$\frac{\partial r}{\partial t}(\mathbf{x},\mathbf{t}) + div(r,\dot{u}) = 0 \quad \text{and} \quad \det(\mathbf{F}) = J = 1 \text{ ----------------------------------(2)}$$

$$E_{ij} = \frac{1}{2}\left[\frac{\partial u_i}{\partial X_j} + \frac{\partial u_j}{\partial X_i} + \frac{\partial u_k}{\partial X_i}\frac{\partial u_k}{\partial X_j}\right] \quad \text{and} \quad \frac{\partial u_i}{\partial X_j} = \frac{\partial N^{(k)}}{\partial \eta}\cdot\frac{\partial \eta}{\partial X_j}u_i^{(k)} \text{ -----------(3)}$$

Figure 3 and 4 show 2D strain visualization ($2E_{12}$, E_{11} and E_{22}) of two bearings with shape factors 12.5 and 4.16 respectively. Compressive load is equal to 1471.5 KN (constant during shear loading). The graphs on the right hand side of each figure show a comparison of results of displacements in which both bearings were sheared until failure occurred.

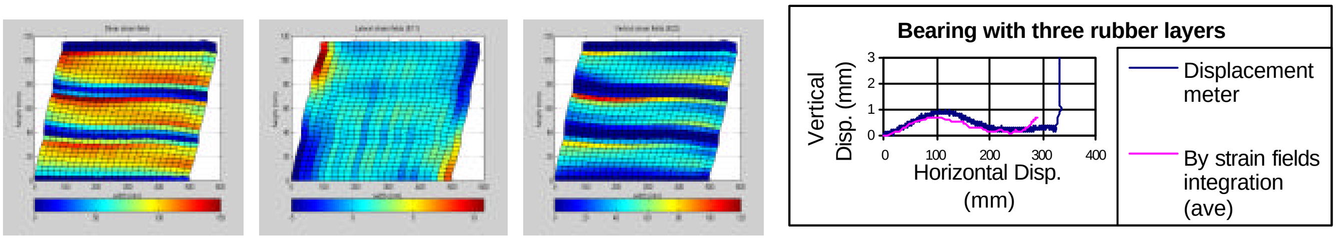

***Figure3:** Strain components three rubber layer (each 30 mm) bearing [maximum shear disp.= 96 mm]*, Displacements comparison chart

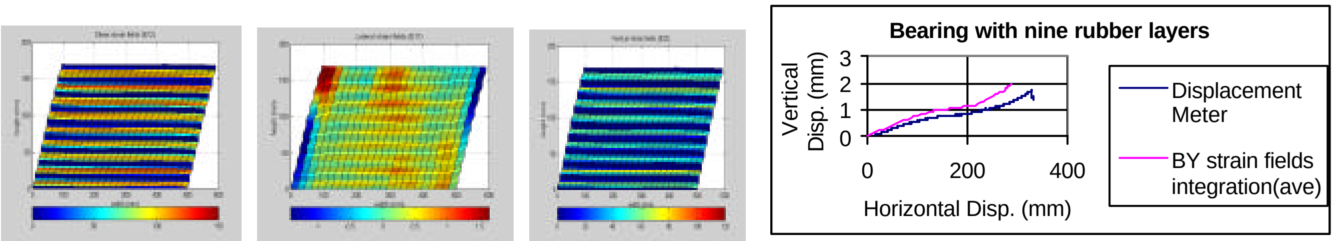

***Figure4**: Strain components nine rubber layer (each 10 mm) bearing [maximum shear disp.= 96 mm), Displacements comparison chart*

Results and Discussion

Comparison of both displacements obtained from the displacement meters and average maximum displacements by strain fields integration show reasonable agreement. Difference in results may be due to in-adequacy of the field measurement system by displacement meter. At large displacements, difference is higher due to error accumulation, which depends on the number of images analyzed and a pixel size. Clearly, different strain component variation indicates that strain localization phenomena occur at each loading step. This variation basically depends on the shape factor and the type of loading. Under compressive loading, maximum shear strain occurs at edges and during shearing it tends to spread to the middle portion, but the maximum still tends to occur at edges. Even though the lateral strain variation is negligible, it visualize that material behavior of most probable area of fracture occurs. This phenomenon is the foundation for defining the failure criterion of rubber bearings which is under development.

Conclusion

Determination of displacement fields of bearing deformation by means of image analysis was developed and tested. It is necessary to consider the strain localization phenomenon to evaluate the mechanical behavior and failure criterion.

References

1. Murat G., Tuncer B.E., Peter J.B., (1999). " Measurement of Particle Movement in Granular Soils Using Image Analysis." Computing in Civil Engineering, 13(2), 116-122.
2. Giachetti A., (2000). "Matching Techniques to Compute Image Motion." Image and vision computing, 18, 247-260.
3. Raffel, M., Willert, C.E., Kompenhans, J., (1998), "Particle Image Velocimetry: A practical guide." Springer, Berlin, New York, 105-146.